

## Closure of the Proterozoic Mozambique Ocean was instigated by a late Tonian plate reorganization event



Alan S. Collins <sup>1✉</sup>, Morgan L. Blades<sup>1</sup>, Andrew S. Merdith<sup>2</sup> & John D. Foden <sup>1</sup>

Plate reorganization events involve fundamental changes in lithospheric plate-motions and can influence the lithosphere-mantle system as well as both ocean and atmospheric circulation through bathymetric and topographic changes. Here, we compile published data to interpret the geological record of the Neoproterozoic Arabian-Nubian Shield and integrate this with a full-plate tectonic reconstruction. Our model reveals a plate reorganization event in the late Tonian period about 720 million years ago that changed plate-movement directions in the Mozambique Ocean. After the reorganization, Neoproterozoic India moved towards both the African cratons and Australia-Mawson and instigated the future amalgamation of central Gondwana about 200 million years later. This plate kinematic change is coeval with the breakup of the core of Rodinia between Australia-Mawson and Laurentia and Kalahari and Congo. We suggest the plate reorganization event caused the long-term shift of continents to the southern hemisphere and created a pan-northern hemisphere ocean in the Ediacaran.

<sup>1</sup>Tectonics and Earth Systems (TES), Department of Earth Sciences, The University of Adelaide, Adelaide, SA, Australia. <sup>2</sup>UnivLyon, Université Lyon 1, Ens de Lyon, CNRS, UMR 5276 LGL-TPE, Villeurbanne, France. ✉email: [alan.collins@adelaide.edu.au](mailto:alan.collins@adelaide.edu.au)

Plate tectonics is characterized by periods of gradual, broadly continuous, plate movement that are punctuated by relatively short times of plate reorganization<sup>1,2</sup>. These are due to the consumption of an oceanic plate, the collision of two continents, the cessation of subduction, or the breakup of a (super)continent<sup>3,4</sup>. These events disturb the plate kinematic status quo and force adjustments over the planet surface that affect ocean and atmospheric circulation and have been linked to perturbations in the carbon cycle<sup>5</sup>, amongst other things. Identifying and understanding plate reorganization events in deep time is only possible with full-plate topological reconstructions. These are well developed for the Mesozoic and younger<sup>6</sup>, but have only recently been proposed for the Paleozoic<sup>7,8</sup> and now Neoproterozoic eras<sup>9,10</sup>. These allow regional plate tectonic induced phenomena to be understood in a global context.

Here we present an updated GPlates ([www.gplates.org](http://www.gplates.org)) model that uses recently published geological data from the terranes of the Arabian-Nubian Shield (ANS). By adding in geological data from relic volcanic arcs into these full-plate topological reconstructions of the ancient earth, we provide a new interpretation of the oceanic plate kinematic and dynamic evolution of the Neoproterozoic Mozambique Ocean. This led to the southward journey of Neoproterozoic India to collide against African Gondwana and the Australia-Mawson continent<sup>11</sup> to form the kernel of Gondwana. This plate reorganization is coeval with the opening of the Pacific Basin<sup>12,13</sup> and directly precedes the cataclysmic climatic perturbations of the Cryogenian.

## Background

Plate tectonics has been causally linked to the Cryogenian climate instability<sup>14–16</sup>, to the coeval Neoproterozoic Oxygenation

Event<sup>17,18</sup>, to the biosphere tumult that included the ecological takeover of eukaryote cells<sup>19,20</sup> and, ultimately, to the evolution of metazoans<sup>21,22</sup>. The veracity of these hypotheses requires knowledge of the plate tectonic configuration and kinematics through the Neoproterozoic, which is missing, as most attempted reconstructions are “continental-drift” models with no full-plate circuit attempted<sup>11,23</sup>. A first attempt at a full-plate topological model for 1000–520 Ma was recently published<sup>9</sup>. However, this model focused predominantly on cratonic crust that had available palaeomagnetic data, and consequently simplified many complex areas around Neoproterozoic active margins. Mallard et al.<sup>24</sup> demonstrated that active margins control plate size and number, therefore also control many of the parameters needed to understand the role of plate tectonics on broader earth systems. The ANS was an active margin and one of these areas simplified in Merdith et al.<sup>9</sup>, yet, it is one of the most critical for Neoproterozoic plate reconstructions as it is one of the most extensive areas of new Neoproterozoic crust on the planet<sup>25</sup> (Fig. 1) and preserves evidence of subduction from pre-1 Ga until the Ediacaran<sup>26</sup>.

The end of the Proterozoic eon is marked by some of the most dramatic events in Earth’s history, with this period of time being characterized by extensive changes in seawater chemistry demonstrated through the strontium, sulfur and carbon isotope records, large climatic extremes, and preservation of the Ediacaran faunal assemblage and the explosion of Cambrian fauna<sup>27</sup>. These global variations are concurrent with the amalgamation of Gondwana, and the closure of the Mozambique Ocean; representing one of the major and final Gondwana forming collisional zones<sup>28</sup>. As no in situ oceanic crust exists before ca. 200 Ma, the remnants of this major ocean gateway are only preserved in relic arc–arc, arc–continent, and continent–continent collisional zones, within the East African Orogen (EAO). The EAO is one of

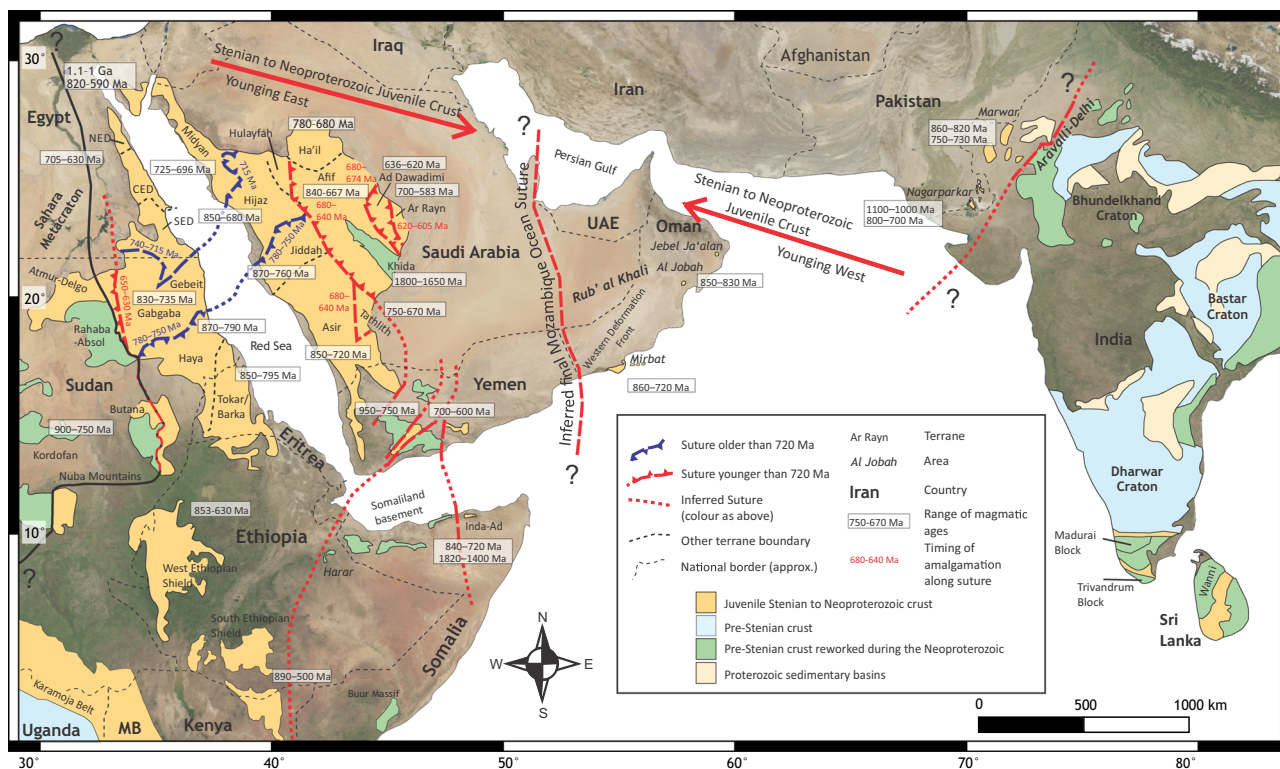


**Fig. 1** Map of present northern Indian Ocean region. Showing the distribution of juvenile Stenian–Ediacaran crust, pre-Stenian exposed crust, pre-Stenian exposed crust reworked thermally and structurally during the Neoproterozoic, and Proterozoic sedimentary basins in NE Africa, Arabia, and the Indian subcontinent. The late Tonian plate reconfiguration is represented by the notable change from pre-720 Ma, approximately NE–SW sutures to post-720 Ma, approximately NNW–SSE striking sutures. MB Mozambique Belt, NED Northern Eastern Desert, CED Central Eastern Desert, SED South Eastern Desert.

the largest orogens of the last billion years, which, in a reconstructed Gondwana, extends from Turkey and the Levant, in the north to Mozambique, Madagascar, Sri Lanka, and East Antarctica in the south<sup>29</sup>. Along strike, the orogen is divided into two. The Mozambique Belt lies in the south and is a tract of largely older continental crust, extensively deformed and metamorphosed in the Neoproterozoic/Cambrian<sup>30</sup>. The ANS makes up the north of the orogen<sup>26</sup>. The ANS, and adjacent Gondwanan rocks in North Africa and from east Arabia to NW India preserve the evidence we use to reconstruct the plate tectonic circuit as Neoproterozoic India converged and finally collided with the African parts of Gondwana<sup>26</sup>.

## Results and Discussion

**Model constraints.** In this paper, we use previously published geological data to constrain our full-plate topological model for the evolution and closure of the Mozambique Ocean and the amalgamation of central Gondwana. The full-plate model is based on geological and paleomagnetic data and is part of the first published self-consistent model of global plate tectonics over the last billion years<sup>10</sup>. We emphasize that this is a model, and although we argue that it best represents the geological and paleomagnetic data available in 2021, it is not a unique solution and is subject to improvement with more data and better interpretations. The model, however, does present interesting implications for the progression of plate tectonics over this time, the distribution of plates, of continents and oceans and leads to hypotheses for plate tectonic influence of earth-surface systems that we begin to explore in this paper.

The ANS is laced with suture zones that represent collisions between different terranes as subduction zones consumed the intervening oceanic crust (Fig. 1). A dramatic feature of the region is that pre-715 Ma sutures are aligned approximately ninety degrees from post-715 Ma sutures<sup>26,31</sup>. This observation reflects a major change in plate convergence direction and we use this as the start of a higher-order reconstruction of this region in a full-plate context.

**The Mozambique Ocean, Azania, and Afif-Abas.** The Mozambique Ocean closed as Neoproterozoic India converged on the African parts of Gondwana (Kalahari, Congo, Sahara) to form central Gondwana<sup>29</sup>. The East African Orogen resulted from the collision between these major continents and amalgams of smaller terranes, during the Neoproterozoic to early Cambrian. Sandwiched within the EAO lies a broad band of Archean to Paleoproterozoic crust that was identified by Collins and Windley<sup>32</sup> as a microcontinent (subsequently named “Azania”), whose remains are found in southern India, central Madagascar, Somalia, eastern Ethiopia, and Arabia (Fig. 1). In Yemen, the Al-Mafid Terrane is correlated with Azania<sup>32</sup> and this is separated from a second pre-Neoproterozoic terrane called the Abas Terrane by a Neoproterozoic arc terrane (the Al Bayda terrane). Because of this, Collins and Windley<sup>32</sup> suggested that a second microcontinent existed that they called Afif-Abas due to the continuation of the Abas terrane into Saudi Arabia as the Afif Terrane.

Azania, and Afif-Abas, are interpreted to have collided with the eastern margins of the Congo craton and Saharan Metacraton by ~630 Ma to form the East African Orogeny *sensu stricto*. A younger orogeny (ca. 570–520 Ma), was interpreted to represent the final collision between India and the amalgamated Africa/Arabia and called the Malagasy orogeny<sup>11</sup>.

**The Eastern Margin of the EAO (NW India to Oman).** The easternmost margin of the northern East African Orogen is the boundary between the Mesoproterozoic terranes of India and the Stenian–Tonian crust that extends west from the Delhi-

Aravalli Orogen. This has been interpreted to be the eastern margin of the northern East African Orogen. During the Stenian and Tonian, progressive arc accretion of volcanic arc rocks onto the NW margin of Neoproterozoic India occurred; extending into the basement rocks of Pakistan and the inliers of Oman<sup>33,34</sup>. This was later covered by an extensive Cryogenian–Ediacaran passive margin succession, with comparable sequences continuing into the Cambrian<sup>35</sup>.

**The Arabian-Nubian Shield.** The ANS is dominated by low grade volcano-sedimentary sequences and associated plutonic and ophiolitic remnants. The tectonic history of the ANS is complicated and preserves a complex mix of terranes, accreted arcs that record subduction polarity reversals that are reviewed and summarized in a number of papers<sup>26,31</sup>. There are no reliable paleomagnetic data available to constrain these blocks, so we have constrained their positions by their relation to each other and through plate kinematic constraints.

The oldest terrane in the ANS is the late Mesoproterozoic Sa'al Metamorphic complex (1.03–1.02 Ga) in Sinai, marking the initiation of magmatism in the northern-most ANS<sup>36,37</sup> (Fig. 1). The location of this Stenian terrane in the reconstruction is uncertain, but coeval subduction-magmatism occurred within the Saharan Metacraton (see below).

The Tonian to Cryogenian history of the ANS is marked by formation of oceanic volcanic arcs and continental volcanic arcs built on Azanian (or Afif-Abas) crust that amalgamated to form a larger intra-Mozambique ocean terrane separate from both Neoproterozoic India and African Gondwanan continents. A number of terranes in the ANS are correlated as equivalents, separated by the opening of the Red Sea, from south to north, these are the Asir and Tokar/Barka terranes, the Haya and Jiddah terranes, the Hijaz and Gabgaba/Gebeit terranes, and the Eastern Desert and Midyan terranes<sup>26</sup>. It is unclear whether the combined Asir-Tokar/Barka terrane and Haya-Jiddah terranes were ever on separate plates as, in Saudi Arabia, no clear suture is seen between them. In SE Sudan and Eritrea, the Barka suture does appear as the site of ocean closure, so these may form a complex middle Tonian amalgam.

The older, Tonian to earliest Cryogenian, amalgamation history of the ANS is marked by approximately NE–SW oriented sutures (present orientation) between juvenile Neoproterozoic ocean-arc terranes. The oldest of these sutures is between the Jiddah-Haya and Gabgaba/Gebeit-Hijaz terranes (the Bi'r Umq–Nakasib suture), and is dated at ca. 780–750 Ma<sup>26</sup>. This suture created the kernel of a late Tonian microcontinent. The Midyan–Eastern Desert collided with this kernel ca. 715 Ma along the Yanbu–Sol Hamed suture<sup>31</sup>. Both of these sutures evolved from SE-dipping subduction zones<sup>31</sup>.

The older NE–SW sutures are bound by younger NNW–SSE Cryogenian to Ediacaran sutures and terranes that represent a fundamental kinematic change in Mozambique Ocean subduction. The oldest of these is the 680–640 Ma Nabitah suture, which forms the eastern margin of the intra-Mozambique Ocean island-arc terrane microcontinent (discussed above), against Tonian–Cryogenian continental arcs built on the Afif-Abas microcontinent. This now enlarged Cryogenian Afif-Abas microcontinent collided with the active margin of the Sahara Metacraton along the Sudanese Keraf Suture. This collision occurred in late Cryogenian to early Ediacaran times (ca. 650–580 Ma)<sup>38</sup>. Further to the east, in the most easterly exposed terrane, the Saudi Ar Rayn Terrane, juvenile calc-alkaline magmatism stretches from ca. 690 to 615 Ma<sup>39</sup>. Turbiditic sediment deposition in the Ad Dawadimi basin that separates the Ar Rayn Terrane from the Afif-Abas microcontinent continued

until at least 620 Ma, but was locally intruded by ca. 630 Ma adakitic magmas<sup>40</sup>. This sequence was metamorphosed to greenschist-facies grades at ca. 620 Ma<sup>41</sup>. Further east still, broad N–S magnetic highs, beneath the Arabian Phanerozoic sedimentary sequence<sup>42</sup>, suggest younger arc terranes now buried beneath the Rub al-Khali Basin. The transition to post-tectonic magmatism within the eastern terranes of the ANS begins from 605 Ma<sup>39</sup> and pull-apart basins developed along the large strike-slip faults that cut the region<sup>43</sup>. Post-tectonic magmatism begins in western Ethiopia at ca. 572 Ma<sup>44</sup>.

The final collision between Neoproterozoic India and the, by then amalgamated, Azania/Congo Craton occurred at ca. 570–540 Ma, closing the final strand of the Mozambique Ocean<sup>11,28</sup>. This suture lies beneath the Phanerozoic cover between the exposed Saudi and Yemen basement and Mirbat in SW Oman. It appears to be imaged by shear-wave anisotropy variations seen directly west of Mirbat<sup>45</sup>. In western Oman, latest Ediacaran–Cambrian deformation is seen in the subsurface, its limit is known as the Western Deformation Front and the deformation associated with this is known as the “Angudan event”. The sub-Rub al-Khali suture has been traced south within reconstructed Gondwana to Madagascar where it has been correlated with the Antsaba shear zone of NW Madagascar<sup>46</sup>, the Betsimisaraka suture<sup>32</sup> and into the Palghat–Cauvery Suture of southern India<sup>47</sup>. This Palghat–Betsimisaraka–Antsaba–Western Deformation Front suture represents the final suture of the Mozambique Ocean<sup>9,11</sup>.

**The Western Margin of the EAO (the eastern Saharan Metacraton).** The Saharan Metacraton is still very poorly known, but

extensive late Mesoproterozoic subduction-related magmatism is found in Chad and west and north Sudan<sup>48</sup>. To the west of this, in eastern Sudan and western Ethiopia magmatism associated with early Neoproterozoic subduction characterizes terranes that are thought to have formed over westward dipping subduction zones<sup>44,49</sup>. This longevity of subduction, which also includes that seen in the Sinai<sup>36,37</sup>, demonstrates that the EAO extends back into the Stenian, or even earlier, when terrane accretion and subduction-zone magmatism initiated against the Paleoproterozoic kernel of the “metacraton”. The NE margin of the Congo Craton, in Uganda, preserves orogenesis that begins with Tonian subduction-zone magmatism in the Karamoja Belt that is coeval with terranes in Sudan<sup>50</sup>.

### A Late Tonian Plate Reconfiguration

The model presented here (Fig. 2) is developed from the reconstruction of Merdith et al.<sup>9</sup>. Details of both geological and paleomagnetic data used to constrain cratonic configurations, positions, and motions are provided therein. Here, data and observations discussed above for the terranes of northern Africa, Arabia, and NW India have been integrated<sup>10</sup>. These define a marked change in Mozambique Ocean subduction kinematics at ca. 720 Ma, from a predominately N–S to E–W striking subduction system (Fig. 2). The timing of these observed changes are broadly coeval with the start of Neoproterozoic India’s southern progression from polar regions to lower latitudes<sup>29,51,52</sup> and we suggest that they represent a plate reorganization in this hemisphere. This kinematic shift is coeval with sedimentological and kinematic estimates for the breakup of the core of Rodinia. The

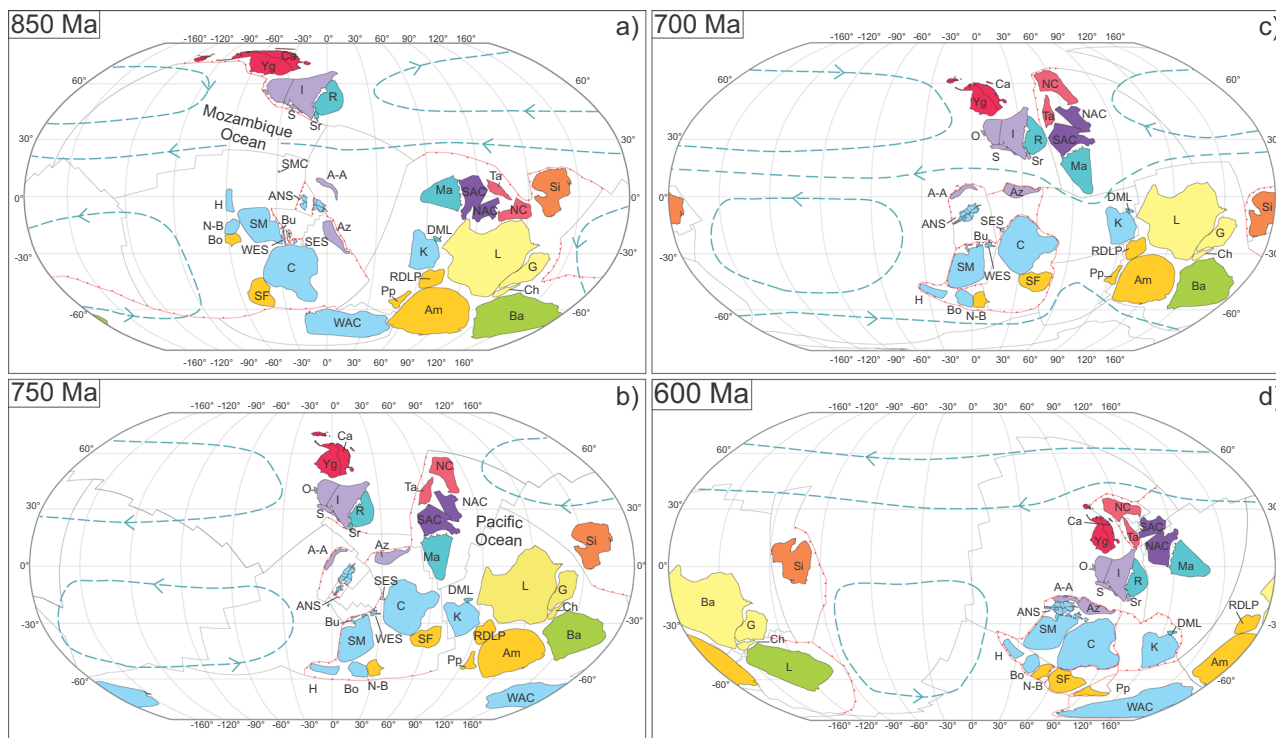


**Fig. 2 Global full-plate topological reconstructions.** **a** 850 Ma, **b** 750 Ma, **c** 700 Ma, **d** 600 Ma modified from Merdith et al.<sup>9,10</sup>, focusing on detail within the ANS. A–A Afif-Abas, Am Amazonia, ANS Arabian-Nubian Shield terrane, Az Azania, Ba Baltic, Bo Borborema, Bu Butana, C Congo, Ca Cathaysia, Ch Chortis, DML Dronning Maud Land, G Greenland, H Hoggar, I Neoproterozoic India, K Kalahari, L Laurentia, Ma Mawson, NAC North Australian Craton, N–B Nigeria-Benin, NC North China, O Oman, Pp Paranapanema, R Rayner, RDLP Rio de la Plata, S Seychelles, SM Sahara Metacraton, SF Saõ Francisco, SMC Sa’al Metamorphic Complex, Sr Sri Lanka, Si Siberia, SAC South Australian/West Australian Craton, SES South Ethiopian Shield, Ta Tarim, WAC West African Craton, WES West Ethiopian Shield, Yg Yangtze. Colors refer to modern continents that the terranes now make up: Red = Asia, Blue = Africa, Gold = South America, Green = Europe, Yellow = North America, Purple = Australia, Teal = Antarctica, Lilac = India, Madagascar, and eastern Arabia. Blue dashed lines indicate schematic ocean currents.

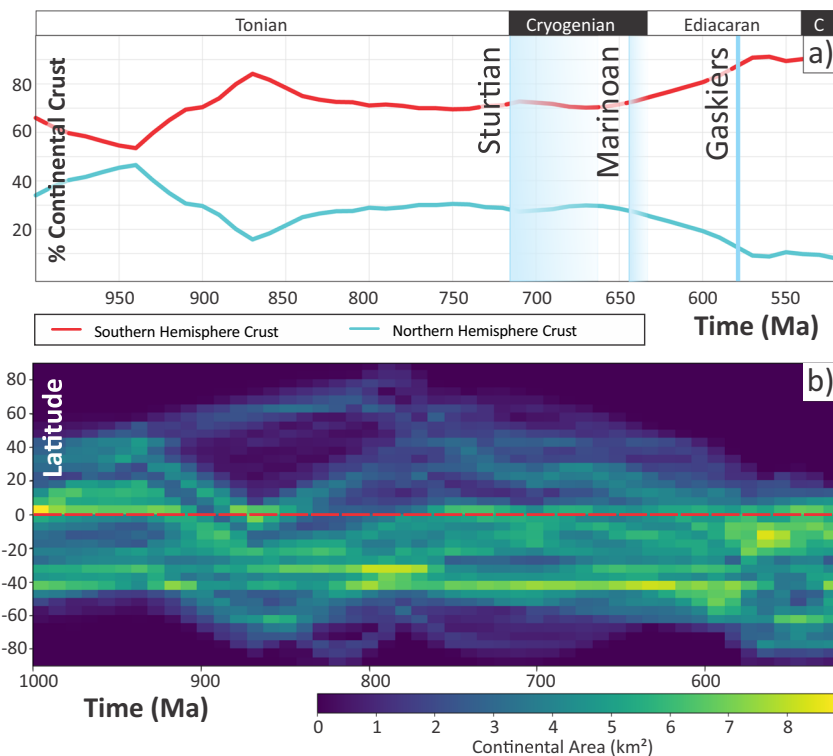


**Fig. 3** Latitudinal distribution of continental crust with respect to time. **a** Percentage of continental crust in either hemisphere as a function of time. Sturtian 717–663 Ma,<sup>57,58</sup> Marinoan 645–635 Ma,<sup>15</sup> and Gaskiers 579 Ma,<sup>54</sup> glacial durations indicated. **b** Histograms of latitudinal distribution of continental area with respect to time (Ma). Both as implied in Merdith et al.<sup>10</sup>. If these models reflect reality, the late Tonian sees the beginning of a long-term trend in continental crust moving to southern latitudes, first into tropical regions through the Cryogenian, promoting a high albedo world. The Ediacaran sees a shift to lower latitudes, which would suppress albedo. C Cambrian.

ancestral Pacific basin is constrained to open before 725 Ma based on kinematic constraints<sup>12</sup> and separation of the Kalahari and Congo continents is also consistent with voluminous magmatism along the southern Congo margin at ca. 750 Ma<sup>53</sup>. This late Tonian plate reorganization heralds the start of a shift of continental crust away from the northern hemisphere into the southern hemisphere (Figs. 2 and 3). This narrows, then eventually closes the equatorial Mozambique Ocean. The model implies that most continental blocks were concentrated in the southern hemisphere in the Late Neoproterozoic (Fig. 3). If this reflects the real distribution, then it would have interesting consequences for ocean/atmosphere circulation. One possible effect would be to compartmentalize ocean gyres in the southern hemisphere, while removing obstacles for hemispherical circulation in the northern hemisphere (Fig. 2). This shift from bi-hemisphere continent distribution towards a world with a pan-northern hemisphere ocean and continents concentrated in the southern hemisphere coincides with end of whole-earth glaciations that characterize the middle Neoproterozoic. In contrast to the Sturtian and Marinoan whole-earth glaciations, Ediacaran glaciations, such as the Gaskiers glaciation, appear more regional in scale<sup>15,54</sup>. Williams and Schmidt<sup>55</sup> hypothesized that the mid-Ediacaran Shuram/Wonoka negative carbon isotope anomaly represents an unprecedented perturbation of the world ocean. We speculate that the plate tectonic driven bifurcation of the planet into continent and ocean latitudinal hemispheres may be a major control on this oceanic perturbation and climate switch—a consequence of the late Tonian plate reorganization.

## Methods

This manuscript is based on a full-plate tectonic reconstruction of the last billion years that has been developed on the open access software GPlates ([www.gplates.org](http://www.gplates.org)).

All GPlates files needed to reconstruct the model are available here—<https://zenodo.org/record/3647901>. The methodology for constructing full-plate tectonic reconstructions are detailed in Merdith et al.<sup>10</sup> and also in Domeier and Torsvik<sup>56</sup>. Computation of latitudinal surface area was done using pyGplates ([www.pygplates.org](http://www.pygplates.org)). To extract the latitudinal distribution of continent area, we first created a global equal-area mesh. We then used a grid-intersection between the nodes of the mesh and the polygons of the plate model that represent continental crust to estimate the area of crust at each latitude. These were summed for each timestep to create an array from 1000–520 Ma of the latitudinal distribution of crust on the earth.

## Data availability

Data derived from the full-plate reconstructions used here to evaluate the latitudinal distribution of continental crust through time are publically available at [https://github.com/amer7632/Collins\\_2021\\_Geology\\_paleaolat](https://github.com/amer7632/Collins_2021_Geology_paleaolat)

## Code availability

The code used to calculate and construct Fig. 3 it is available here: [https://github.com/amer7632/Collins\\_2021\\_Geology\\_paleaolat](https://github.com/amer7632/Collins_2021_Geology_paleaolat)

Received: 1 June 2020; Accepted: 16 March 2021;

Published online: 20 April 2021

## References

- Gordon, R. G. & Jurdy, D. M. Cenozoic global plate motions. *J. Geophys. Res. Solid* **91**, 2389–2406 (1986).
- Muller, R. D. et al. Ocean basin evolution and global-scale plate reorganization events since Pangea breakup. *Ann. Rev. Earth Planet. Sci.* **44**, 107–138 (2016).
- Austermann, J. et al. Quantifying the forces needed for the rapid change of Pacific plate motion at 6 Ma. *Earth Planet. Sci. Lett.* **307**, 289–297 (2011).
- Whittaker, J. M. et al. Major Australian–Antarctic plate reorganization at Hawaiian–Emperor bend time. *Science* **318**, 83–86 (2007).

5. Louis-Schmid, B. et al. Detailed record of the mid-Oxfordian (Late Jurassic) positive carbon-isotope excursion in two hemipelagic sections (France and Switzerland): a plate tectonic trigger? *Palaeogeogr. Palaeoclimatol. Palaeoecol.* **248**, 459–472 (2007).
6. Muller, R. D. et al. A global plate model including lithospheric deformation along major rifts and orogens since the Triassic. *Tectonics* **38**, 1884–1907 (2019).
7. Domeier, M. A plate tectonic scenario for the Iapetus and Rheic oceans. *Gondwana Res.* **36**, 275–295 (2016).
8. Domeier, M. & Torsvik, T. H. Plate tectonics in the late Paleozoic. *Geosci. Front.* **5**, 303–350 (2014).
9. Meredith, A. S. et al. A full-plate global reconstruction of the Neoproterozoic. *Gondwana Res.* **50**, 84–134 (2017).
10. Meredith, A. S. et al. Extending full-plate tectonic models into deep time: linking the Neoproterozoic and the Phanerozoic. *Earth-Sci. Rev.* **214**, 103477 (2021).
11. Collins, A. & Pisarevsky, S. Amalgamating eastern Gondwana: the evolution of the circum-Indian orogens. *Earth-Sci. Rev.* **71**, 229–270 (2005).
12. Meredith, A. S., Williams, S. E., Muller, R. D. & Collins, A. S. Kinematic constraints on the Rodinia to Gondwana transition. *Precambrian Res.* **299**, 132–150 (2017).
13. Lloyd, J. C. et al. Neoproterozoic geochronology and provenance of the Adelaide Superbasin. *Precambrian Res.* **350**, 105849 (2020).
14. Gernon, T. M., Hincks, T. K., Tyrrell, T., Rohling, E. J. & Palmer, M. R. Snowball Earth ocean chemistry driven by extensive ridge volcanism during Rodinia breakup. *Nat. Geosci.* **9**, 242–U283 (2016).
15. Hoffman, P. F. et al. Snowball Earth climate dynamics and Cryogenian geology-geobiology. *Sci. Adv.* **3**, e1600983 (2017).
16. Sobolev, S. V. & Brown, M. Surface erosion events controlled the evolution of plate tectonics on Earth. *Nature* **570**, 52 (2019).
17. Li, C., Cheng, M., Zhu, M. & Lyons, T. W. Heterogeneous and dynamic marine shelf oxygenation and coupled early animal evolution. *Emerging Top. Life Sci.* **2**, 279–288 (2018).
18. Williams, J. J., Mills, B. J. W. & Lenton, T. M. A tectonically driven Ediacaran oxygenation event. *Nat. Commun.* **10**, 2690 (2019).
19. Lenton, T. M., Boyle, R. A., Poulton, S. W., Shields-Zhou, G. A. & Butterfield, N. J. Co-evolution of eukaryotes and ocean oxygenation in the Neoproterozoic era. *Nat. Geosci.* **7**, 257–265 (2014).
20. Brocks, J. J. et al. The rise of algae in Cryogenian oceans and the emergence of animals. *Nature* **548**, 578 (2017).
21. Sahoo, S. K. et al. Ocean oxygenation in the wake of the Marinoan glaciation. *Nature* **489**, 546–549 (2012).
22. McKenzie, N. R., Hughes, N. C., Gill, B. C. & Myrow, P. M. Plate tectonic influences on Neoproterozoic-early Paleozoic climate and animal evolution. *Geology* **42**, 127–130 (2014).
23. Li, Z. X. et al. Assembly, configuration, and break-up history of Rodinia: a synthesis. *Precambrian Res.* **160**, 179–210 (2008).
24. Mallard, C., Coltice, N., Seton, M., Muller, R. D. & Tackley, P. J. Subduction controls the distribution and fragmentation of Earth's tectonic plates. *Nature* **535**, 140 (2016).
25. Stern, R. A. Crustal evolution in the East African Orogen: a neodymium isotopic perspective. *J. Afr. Earth Sci.* **34**, 109–117 (2002).
26. Johnson, P. R. et al. Late Cryogenian-Ediacaran history of the Arabian-Nubian Shield: a review of depositional, plutonic, structural, and tectonic events in the closing stages of the northern East African Orogen. *J. Afr. Earth Sci.* **61**, 167–232 (2011).
27. Halverson, G. P., Hurtgen, M., Porter, S. M. & Collins, A. S. in *Events at the Precambrian-Cambrian boundary: a focus on southwestern Gondwana* (eds. Gaucher, C., Sial, A., Halverson, G. P. & Frimmel, H.) (Elsevier, 2010).
28. Schmitt, R. d. S., Fragoso, R. d. A. & Collins, A. S. in *Geology of Southwest Gondwana* (eds. Siegfried S., Miguel A. S. B., Pedro O. & Sebastian O.) (Springer International Publishing, 2018).
29. Meert, J. G. A synopsis of events related to the assembly of eastern Gondwana. *Tectonophysics* **362**, 1–40 (2003).
30. Fritz, H. et al. Orogen styles in the East Africa Orogens: a review of the Neoproterozoic to Cambrian tectonic evolution. *J. Afr. Earth Sci.* **86**, 65–106 (2013).
31. Robinson, F. A., Foden, J. D. & Collins, A. S. Geochemical and isotopic constraints on island arc, synorogenic, post-orogenic and anorogenic granitoids in the Arabian Shield, Saudi Arabia. *Lithos* **220**, 97–115 (2015).
32. Collins, A. & Windley, B. The tectonic evolution of central and northern Madagascar and its place in the final assembly of Gondwana. *J. Geol.* **110**, 325–339 (2002).
33. Alessio, B. L. et al. Origin and tectonic evolution of the NE basement of Oman: a window into the Neoproterozoic accretionary growth of India? *Geol. Mag.* **155**, 1150–1174 (2018).
34. Blades, M. L. et al. Unravelling the Neoproterozoic accretionary history of Oman, using an array of isotopic systems in zircon. *J. Geol. Soc.* <https://doi.org/10.1144/jgs2018-125> (2019).
35. Cozzi, A., Rea, G. & Craig, J. From global geology to hydrocarbon exploration: Ediacaran-early Cambrian petroleum plays of India, Pakistan and Oman. *Geol. Soc. Spec. Publ.* **366**, 131–162 (2012).
36. Be'eri-Shlevin, Y., Eyal, M., Eyal, Y., Whitehouse, M. J. & Litvinovsky, B. The Sa'al volcano-sedimentary complex (Sinai, Egypt): a latest Mesoproterozoic volcanic arc in the northern Arabian Nubian Shield. *Geol.* **40**, 403–406 (2012).
37. Eyal, M., Be'eri-Shlevin, Y., Eyal, Y., Whitehouse, M. J. & Litvinovsky, B. Three successive Proterozoic island arcs in the Northern Arabian-Nubian Shield: evidence from SIMS U-Pb dating of zircon. *Gondwana Res.* **25**, 338–357 (2014).
38. Abdelsalam, M. G. et al. The Neoproterozoic Keraf Suture in NE Sudan: sinistral transpression along the eastern margin of West Gondwana. *J. Geol.* **106**, 133–147 (1998).
39. Doebrich, J. L. et al. Geology and metalogeny of the Ar Rayn terrane, eastern Arabian shield: evolution of a Neoproterozoic continental-margin arc during assembly of Gondwana within the East African orogen. *Precambrian Res.* **158**, 17–50 (2007).
40. Cox, G. M., Foden, J. & Collins, A. S. Late Neoproterozoic adakitic magmatism of the eastern Arabian Nubian Shield. *Geosci. Front.* **10**, 1981–1992 (2019).
41. Cox, G. M. et al. Ediacaran terrane accretion within the Arabian-Nubian Shield. *Gondwana Res.* **21**, 341–352 (2012).
42. Johnson, P. R. & Stewart, I. C. F. Magnetically inferred basement structure in central Saudi Arabia. *Tectonophysics* **245**, 37–52 (1995).
43. Nettle, D. et al. A middle-late Ediacaran volcano-sedimentary record from the eastern Arabian-Nubian shield. *Terra Nova* **26**, 120–129 (2014).
44. Blades, M. L. et al. Age and hafnium isotopic evolution of the Didesa and Kemashi Domains, western Ethiopia. *Precambrian Res.* **270**, 267–284 (2015).
45. Al-Lazki, A. et al. Upper mantle anisotropy of southeast Arabia passive margin [Gulf of Aden northern conjugate margin], Oman. *Arab. J. Geosci.* **5**, 925–934 (2012).
46. Armistead, S. E. et al. Evolving marginal terranes during Neoproterozoic supercontinent reorganization: constraints from the Bemarivo Domain in Northern Madagascar. *Tectonics* **38**, 2019–2035 (2019).
47. Collins, A. S. et al. Passage through India: the Mozambique Ocean suture, high-pressure granulites and the Palghat-Cauvery shear zone system. *Terra Nova* **19**, 141–147 (2007).
48. de Wit, M. J. & Linol, B. In *Geology and Resource Potential of the Congo Basin* (eds Maarten, J. de Wit, François, G. & Michiel, C. J. de Wit) (Springer, 2015).
49. Blades, M. L., Foden, J., Collins, A. S., Alemu, T. & Woldetinsae, G. The origin of the ultramafic rocks of the Tulu Dimtu Belt, western Ethiopia - do they represent remnants of the Mozambique Ocean? *Geol. Mag.* **156**, 62–82 (2019).
50. Westerhof, A. B. P. et al. *Geology and Geodynamic Development of Uganda with Explanation of the 1:1,000,000 Scale Geological Map.* 387 (Geological Survey of Finland, 2014).
51. Meert, J. G. et al. Precambrian crustal evolution of Peninsular India: a 3.0 billion year odyssey. *J. Asian Earth Sci.* **39**, 483–515 (2010).
52. Powell, C. M. & Pisarevsky, S. A. Late Neoproterozoic assembly of East Gondwana. *Geology* **30**, 3–6 (2002).
53. Hoffman, P. F., Hawkins, D. P., Isachsen, C. E. & Bowring, S. A. Precise U-Pb zircon ages for early Damaran magmatism in the Summas Mountains and Welwitschia Inlier, northern Damara belt, Namibia. *Commun. Geol. Sur. Namibia* **11**, 47–52 (1996).
54. Pu, J. P. et al. Dodging snowballs: geochronology of the Gaskiers glaciation and the first appearance of the Ediacaran biota. *Geology* **44**, 955–958 (2016).
55. Williams, G. E. & Schmidt, P. W. Shuram-Wonoka carbon isotope excursion: Ediacaran revolution in the world ocean's meridional overturning circulation. *Geosci. Front.* **9**, 391–402 (2018).
56. Domeier, M. & Torsvik, T. H. Full-plate modelling in pre-Jurassic time. *Geol. Mag.* **156**, 261–280 (2019).
57. Cox, G. M. et al. South Australian U-Pb zircon (CA-ID-TIMS) age supports globally synchronous Sturtian deglaciation. *Precambrian Res.* **315**, 257–263 (2018).
58. Macdonald, F. A. et al. Calibrating the Cryogenian. *Science* **327**, 1241–1243 (2010).

### Acknowledgements

A.S.C. is supported by Australian Research Council grants FT120100340 and with M.L.B. and J.D.F. are funded by LP160101353, with the support of the Northern Territory Geological Survey, Origin Energy, Santos Ltd and Imperial Oil and Gas. A.S.M. is supported by the Deep Energy Community of the Deep Carbon Observatory. We are grateful for the help of two reviewers who improved the manuscript.

### Author contributions

A.S.C., M.L.B. and J.D.F. conceived of and initiated the project. A.S.M. built the full-plate reconstruction. A.S.C. and M.L.B. co-wrote the first draft of the paper. M.L.B. and A.S.M. interpreted the data. All authors edited, revised, and reviewed the manuscript.

**Competing interests**

The authors declare no competing interests.

**Additional information**

**Supplementary information** The online version contains supplementary material available at <https://doi.org/10.1038/s43247-021-00149-z>.

**Correspondence** and requests for materials should be addressed to A.S.C.

**Peer review information** Primary handling editor: Joseph Aslin.

**Reprints and permission information** is available at <http://www.nature.com/reprints>

**Publisher's note** Springer Nature remains neutral with regard to jurisdictional claims in published maps and institutional affiliations.



**Open Access** This article is licensed under a Creative Commons Attribution 4.0 International License, which permits use, sharing, adaptation, distribution and reproduction in any medium or format, as long as you give appropriate credit to the original author(s) and the source, provide a link to the Creative Commons license, and indicate if changes were made. The images or other third party material in this article are included in the article's Creative Commons license, unless indicated otherwise in a credit line to the material. If material is not included in the article's Creative Commons license and your intended use is not permitted by statutory regulation or exceeds the permitted use, you will need to obtain permission directly from the copyright holder. To view a copy of this license, visit <http://creativecommons.org/licenses/by/4.0/>.

© The Author(s) 2021